Hydrological response to long-lasting dry spell at the southern edge of Siberian permafrost

Li Han [a,b,*], Lucas Menzel [a]

[a] Department of Geography, Heidelberg University, Heidelberg 69120, Germany
[b] Section Hydrology, GFZ German Research Centre for Geosciences, Potsdam 14473, Germany

HIGHLIGHTS

- We investigate the historical hydro-climate variations of dry and wet spells in the semiarid permafrost region.
- Comparative studies reveal concurrent hot and dry conditions in a prolonged dry spell driven by land-atmosphere coupling.
- Warming-induced permafrost degradation intensifies drought dynamics in the coupled land-atmosphere system.
- Our study warns of irreversible freshwater issues in water-scarce semi-arid regions undergoing permafrost loss.

GRAPHICAL ABSTRACT
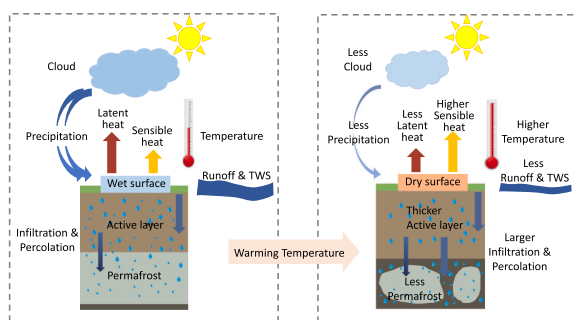
Large-scale permafrost loss induces dry surface that intensifies land-atmosphere coupling

ARTICLE INFO

ABSTRACT

Regions experiencing prolonged dry spell exhibit intensified land-atmosphere coupling, exacerbating dry conditions within the hydrological system. Yet, understanding the propagation of these processes within the context of permafrost degradation remains limited. Our study investigates concurrent hydro-climate variations in the semi-arid Selenga River basin in the southern edge of Siberian permafrost. Driven by the natural atmospheric circulations, this region experienced two distinct dry spells during 1954–2013. It enables comparative investigations into the role of warming-induced permafrost degradations in drought dynamics under land-atmosphere coupling.

Based on a comprehensive analysis of observed borehole data from 1996 to 2009 and empirical methods, we identify widespread permafrost loss in the semi-arid Selenga region. Such large-scale landscape changes may increase the infiltration of water from the surface to the subsurface hydrological system, and significantly influence the dry conditions in landsurface. First, significant decreasing trends are observed in river runoff (-0.30mm/yr, $p < 0.05$) and TWS (-3.16 mm/yr, $p = 0.1$), despite the absence of an apparent trend in annual precipitation (0.009 mm/yr, $p = 0.9$). Furthermore, in comparison to the first dry spell (1974–1983, 10yrs), the hydro-climatic variables show prolonged and more severe water deficits in runoff and TWS during the second dry spell (1996–2012, 17 yrs), with a reduced runoff-generation efficiency from precipitation. Such exacerbated dry conditions are coincident with amplified positive anomalies observed in air temperature, PET, as well as low-level geopotential height. These concurrent "hot-dry" phenomena indicate an enhanced land-atmospheric

* Corresponding author at: Section Hydrology, GFZ German Research Centre for Geosciences, Potsdam 14473, Germany.
  E-mail address: li.han@gfz-potsdam.de (L. Han).

interaction within the hydro-climate system, which is further evidenced by the negative relationship between permafrost thawing index and runoff deficits (regression coefficient = −3.8, p < 0.001). As climate warming continues, the ongoing permafrost degradation could reinforce water scarcity, triggering an irreversible shift in water availability in water-scarce regions. Our findings could support freshwater management for regional food supply, human health, and ecosystem functions in the regions undergoing large-scale permafrost degradation.

1. Introduction

Hydrological drought, a complex and multivariate natural hazard, typically arises from prolonged precipitation deficits, manifesting as abnormal deficiencies in surface and subsurface water systems within the terrestrial hydrological cycle (Van Loon, 2015). Along with a changing climate, droughts are expected to become more frequent, intense, and prolonged, posing severe threats to water-limited regions where the hydrological system is already vulnerable to water scarcity (Cook et al., 2018). The severity and development of hydrological drought are influenced not only by climate drivers, such as the duration and magnitude of precipitation deficiency, but also by catchment-specific characteristics, including moisture storage and release capacity in soil and subsurface systems. Moreover, these climate and landscape characteristics may interact with each other, further complicating the development of hydrological drought (Van Loon, 2015; Miralles et al., 2019). These interactions are particularly prominent during a dry spell, which represents a period of abnormally reduced water availability in the hydrological system.

During a dry spell, the persistent deficiency of precipitation is not able to sustain enough input water to the hydrological system, leading to water scarcity and hydrological droughts, especially in water-limited regions (Slater et al., 2021). As temperature rises, the hydrological cycle is expected to accelerate due to increased actual evapotranspiration (Jung et al., 2010). However, under extremely dry conditions, the lack of available moisture in the land surface and upper soil layers could restrict actual evapotranspiration despite temperature increases (Seneviratne et al., 2006; Miralles et al., 2019). This could lead to a drier moisture condition in the lower atmosphere, suppressing the probability of precipitation and perpetuating a dry state in the land surface (Seneviratne et al., 2010). Concurrently, reduced actual evapotranspiration leads to less latent heat but a larger portion of sensible heat flux that could warm the air through direct radiation, which ultimately induces hotter and drier air condition and a higher likelihood of heatwaves (Miralles et al., 2019). As thus, this enhanced land-atmosphere coupling during dry spells could potentially lead to prolonged hot and dry conditions (Seneviratne et al., 2006; Miralles et al., 2019; Zhang et al., 2020).

Changes in climate and landscape may facilitate the aforementioned drought dynamics (Cook et al., 2018). From climate perspective, variations in precipitation, governed by natural variability of atmospheric circulation, can directly control the occurrence of drought (Trenberth et al., 2014). From landscape perspective, human-induced land degradation (Hermans and McLeman, 2021), such as reduced vegetation coverage (Cook et al., 2009), deforestation (Bagley et al., 2014) and desertification (Mariano et al., 2018), has been found to suppress evapotranspiration and further exacerbate drought severity through intensified positive land-atmosphere feedback. In this study, we focus on another type of landscape evolution, i.e., permafrost degradation, that could influence the drought dynamics.

Permafrost is a frozen soil zone that remains at or below 0 °C for two or more years (Dobinski, 2011; Woo, 2012). It acts as an aquiclude that hinders subsurface water movement due to its low hydraulic conductivity (Woo, 2012). However, in a warming climate, permafrost undergoes significant large-scale degradation, including reduced thickness and extent, and even potential northward migration of the permafrost boundary (Romanovsky et al., 2010; Biskaborn et al., 2019; Smith et al., 2022). These evolutions in landscape may modify the water storage and release capacity of the hydrological system, making catchments underlain by permafrost ideal settings for investigating the response of hydrological drought to climate and landscape changes from a coupled land-atmosphere perspective.

Permafrost degradation enhances pathways connecting surface and subsurface water systems, ultimately altering moisture conditions in the soil and groundwater system (Walvoord and Kurylyk, 2016). In the ice-rich continuous permafrost region, where >90 % of the landscape is underlain by permafrost, a warming environment leads primarily to a vertical degradation that increases the thickness of active layer. In this case, the frozen layer beneath the active layer still serves as an effective barrier that prevents water from percolating deeply. As a result, the active layer can sustain a wet surface or near-surface conditions (Iijima et al., 2014), which can increase the surface runoff but limit the subsurface drainage (Han and Menzel, 2022). However, in the transition regions such as the region investigated in this study, i.e. regions underlain by thin and spatially discontinuous frozen layers, increased permafrost-free areas could allow more water infiltration and percolation into the deeper groundwater system, leading to drier condition in landsurface and near-surface soil moisture during the thawing season (Ishikawa et al., 2005). Although the hydrological consequences of permafrost degradation have been investigated in wetland and lake development in permafrost environments (Jones et al., 2022; Haynes et al., 2018; Boike et al., 2016; Carroll et al., 2011; Smith et al., 2005), the influence of permafrost-degradation-induced drying dynamics on the propagation of hydrological drought remains poorly understood.

In this study, we focus on the Selenga River Basin, located at the southern edge of Siberian permafrost in northern Mongolia. It is situated at the transition belt between the semi-arid and boreal zones and between continuous and discontinuous or sporadic/isolated permafrost zones. The permafrost in this area is experiencing significant degradation due to ongoing warming (Ishikawa et al., 2018; Wu et al., 2022a, 2022b; Wang et al., 2022). Water resources in this region are scarce and vulnerable to changes in climate and landscape (Karthe et al., 2017). Furthermore, the increasing water demand due to a growing population, accelerated urbanization, and the mining industry may potentially exceed the limited water supply in this region (Priess et al., 2011, 2015). This situation ultimately challenges the water-sharing regulation between Mongolia in the upstream and downstream Russia. In addition, the Selenga River is one of the most important tributaries of Lake Baikal, contributing about 50 to 60 % of lake's surface water influx (Chalov et al., 2015; Törnqvist et al., 2014; Kasimov et al., 2020). Therefore, effective management and governance of water-saving technologies, especially during long lasting dry spells, is crucial to ensuring water and food security in this region under the current challenges of climate change, population growth, and aquifer depletion.

Studies based on two-hundred-year tree-ring analysis revealed severe drought conditions during recent decades (Pederson et al., 2014; Zhang et al., 2020), with critical consequences on the ecosystem, such as accelerated carbon depletion and high livestock mortality (Lu et al., 2019; Rao et al., 2015). Furthermore, this region experiences oscillations between dry and wet states due to the natural variability of atmospheric circulation during 1954–2013 (Han and Menzel, 2022), resulting in two distinct dry spells during 1974–1983 and 1996–2012. As the permafrost conditions during these two periods are distinct, they provide an opportunity to compare the drought propagation processes in response to historical evolution in permafrost.

In this study, we propose a hypothesis that, in semi-arid permafrost

regions such as the Selenga catchment, warming-induced large-scale lateral permafrost degradation may trigger a drying loop in the corresponding hydro-climate system. Such an assumption relies on the fact that whole-scale permafrost loss could intensify water infiltration and percolation. Therefore, it could result in a drying surface condition that further enhances land-atmosphere coupling. To elucidate our hypothesis, we first examine the historical variations of key hydro-climate factors, with a special focus on the detection of dry and wet spells. We then identify a concurrent presence of hot and dry conditions within the hydro-climate system during a prolonged dry spell. This phenomenon is also recognized as an intensified land-atmosphere coupling. Subsequently, we explore how permafrost degradation, driven by a warming climate, may enhance drought dynamics in such a coupled land-atmosphere system. Then we relate the long-term and periodical change of Thawing Index (TI) with dry condition in hydrological system. Through such a systematic analysis, our study aims to provide insights into the potential role of permafrost degradation in exacerbating hydrological droughts within the context of land-atmosphere coupling.

2. Study area

The Selenga River catchment is located in the Central Mongolian Plateau (Fig. 1). It covers a number of sub-basins and mountain ranges, with the Khangai and Khentii Mountains, peaking at or above 2800 m a. s.l (Fig. 1a). The total area of the catchment is about 440,000 km^2, about two-thirds of which is in Mongolia and the rest in the Russian Federation (UNDP, 2013). The Selenga catchment is located on the southern edge of the continuous permafrost, gradually transitioning into the discontinuous or sporadic/isolated permafrost (see Fig. 1c). It also lies within the transitional zone between the Siberian taiga and the arid mid-latitudes. The catchment experiences a harsh continental climate, characterized by long cold winters and moderately warm summers (Batima et al., 2005; Törnqvist et al., 2014). During the observation period from 1954 to 2013, the average monthly temperature in July is around +15 °C, while it reaches a minimum of approximately −23 °C in January, based on temperature data from Climatic Research Unit (CRU). Precipitation is the main source of input water to Selenga river (Frolova et al., 2017; Törnros and Menzel, 2010). The total annual precipitation is approximately 310 mm, with over 60 % concentrated in the summer months (Munkhjargal et al., 2020). Snowfall is mainly present from mid-October

to mid-April but it usually only leaves a thin snowcover. In addition to intra-annual variations, both precipitation and air temperature exhibit significant spatial variation between the mountains and depressions during the period 1954–2013, based on data from Global Precipitation Climatology Centre (GPCC) and Climatic Research Unit (CRU). Generally, the mountainous areas in the southwest experience extremely cold and dry climatic conditions, while the valley regions near Lake Baikal are characterized by higher precipitation and a somewhat milder climate.

The landcover of Selenga River catchment exhibits large gradients from south to north (Fig. 1b). The upstream region in the south is dominated by a forest-steppe mosaic (Kopp et al., 2014), while the downstream part in the north is primarily covered by boreal forest but includes some agricultural activities (Klinge et al., 2018). The geological structure in the Selenga basin is also highly complex, characterized by a predominance of magmatic rocks, as well as metamorphic and volcanogenic formations (Kasimov et al., 2020). Specifically, this region is predominantly characterized by various permafrost conditions, with discontinuous permafrost underlying the mountainous regions and sporadic/isolated permafrost occurring in the central region of the basin (Törnqvist et al., 2014), as shown in Fig. 1c. This figure is obtained based on Obu et al. (2019) which represents the permafrost coverage during 2000–2016. For comparison, Fig. S6 based on Gruber (2012) is included to represent the permafrost conditions during the historical period spanning from 1961 to 1990. We note that the differences between these two maps may be an evidence of permafrost degradation, but they might also be a consequence of large uncertainties of the different modeling methods used for each map. Overall, both maps reveal that the Selenga catchment is located in the transition belt between continuous and discontinuous or sporadic/isolated permafrost zones.

3. Datasets and methodology

3.1. Hydrological and climate data

Monthly river runoff data (R) for the Mostovoy gauge station at the outlet of the Selenga River Basin is available from the Global Runoff Data Center (GRDC; in Koblenz, Germany, http://www.bafg.de/GRDC) for the 60 years period during 1954–2013. Since the meteorological station networks in Selenga region is sparse and irregular (Rawlins et al.,
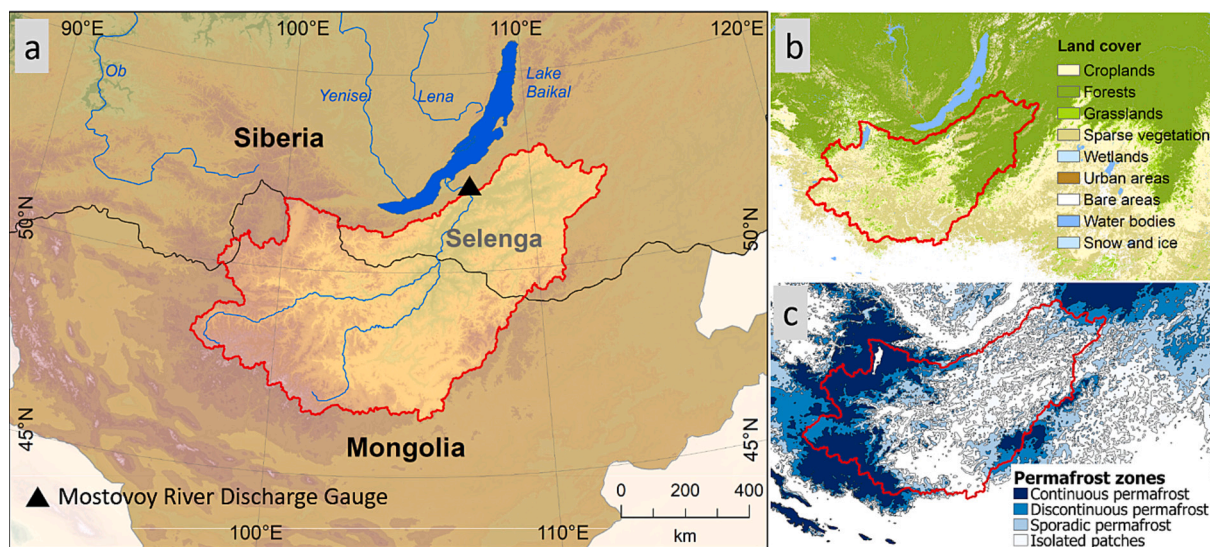

Fig. 1. Landscape characteristics in the Selenga River Basin: (a) basin location and elevation (b) land cover, and (c) permafrost distribution. The land cover data is from Globcover products, which is based on the ESA-Globcover project (http://due.esrin.esa.int/page_globcover.php). The Permafrost Zonation Index (PZI), as introduced by Obu et al. (2019), depicts the distribution of permafrost, such that 90–100 % is considered continuous permafrost, 50–90 % is discontinuous, 10–50 % is sporadic, and < 10 % represents isolated permafrost.

2010), multiple global gridded datasets have been utilized in this study. As there is no long-term data available for the actual evapotranspiration (ET) in this region, the PET data is employed to represent the atmospheric conditions. The precipitation (P) is from the Global Precipitation Climatology Center (GPCC). The air temperature (T) and the potential evapotranspiration (PET) are from Climate Research Unit (CRU). Considering the coarse resolution of the CRU and GPCC data, we conducted comparison analysis between these two gridded data with the GSOD observation data over the available 19 stations in the Selenga catchment (Fig. S1, S2). The regression coefficients between GPCC and GSOD for all stations range from 0.52 to 0.92, with an overall regression slope of 0.93. For CRU temperature data, the regression rates range from 0.93 to 0.96. The average regression between CRU and GSOD data is 0.96 across all 19 stations. These results suggest that both GPCC and CRU data can effectively represent the precipitation and temperature conditions in the Selenga catchment.

We used a reanalyzed dataset GRACE-REC (Humphrey and Gudmundsson, 2019) that contains long-term records of terrestrial water storage (TWS), which provides an individual dataset representing moisture conditions in the terrestrial hydrological system, including the groundwater component. In addition, large-scale atmospheric circulation is characterized by using the geopotential height patterns (850-hPa and 500-hPa) from the National Center for Environmental Prediction-National Center for Atmospheric Research (NCEP-NCAR) reanalysis dataset (Kalnay et al., 1996). As these aforementioned gridded-based datasets are homogeneously processed using the same consistent standards and methodology over both time and space scales, they enable an even estimation over regional scale and with complete temporal coverage. Monthly time series of these hydro-climatic elements have been extracted from each gridded dataset at the basin scale. Additional information, such as spatial resolution, time step, and access details, is provided in Table 1.

3.2. Methods

3.2.1. Indicator of long-term permafrost change

In this study, we employed the Thawing Index (TI) as an indirect signal of large-scale and long-term permafrost degradation. This method relies on the direct thermal response of the land surface to the atmosphere, with a linear relationship between air temperature and ground thermal condition (Nelson and Outcalt, 1987; Zhang et al., 2005). TI is calculated based on Stefan's method (Stefan, 1891), a measure used to quantify the amount of heat accumulated over a year that contributes to the thawing of permafrost (Nelson and Outcalt, 1987; Zhang et al., 2005; Frauenfeld et al., 2007; Peng et al., 2018). This approach was previously described by Frauenfeld et al. (2007):

$$TI = \sum_{i=1}^{M_T} |T_i| \times D_i, \quad T_i \geq 0°C$$

where TI is the summation of the monthly air temperatures if the respective temperature is above the freezing point, i.e. for $i = 1, 2, \ldots M_T$;

T_i is the gridded mean monthly air temperature from the CRU dataset; D_i is the number of days in that month. TI serves as an effective indicator of thermal condition in climate and land surface. Changes in TI reflects the varied spatial distribution of frozen ground (Frauenfeld et al., 2007). It is also worthy to note that TI alone cannot conclusively determine the presence or absence of permafrost. To make such determinations, one may need to consider additional ground factors and measurements for the specific region.

3.2.2. Statistical methods

3.2.2.1. Anomaly analysis.
To elucidate the historical variations in the individual water-related variables, specifically precipitation (P), river runoff (R), and terrestrial water storage (TWS) from their long-term mean values (1954–2013), we derived the respective anomalies for each variable in each year under consideration. Here, negative anomalies of P, R and TWS indicate instances of water deficits or droughts, whereas positive anomalies refer to relatively wet conditions within the hydrological system. The temporal progression of both dry and wet conditions is visually depicted in Fig. 2.

3.2.2.2. Normalized percentiles ranking analysis.
To gain insights into the persistent hot-dry conditions prevalent from 1954 to 2013, our study employs standardized time series of key hydro-climatic variables: precipitation (P), runoff (R), terrestrial water storage (TWS), temperature (T), and potential evapotranspiration (PET). The time series data is organized in an ascending order, with ranks assigned to each value. Ranks are assigned on a scale from 1 to 60 based on the magnitude of the variables, with a rank of 1 representing the lowest recorded value, and a rank of 60 indicating the highest (Tijdeman et al., 2020).

Additionally, we utilize three percentiles (20 %, 50 %, and 80 %) as thresholds to delineate dry and wet (cool and warm) conditions. The 50th percentile serves as the threshold for distinguishing between dry (cool) and wet (warm) periods. Anomalies below 50 % in precipitation, runoff, and TWS suggest dry years, while values above 50 % suggest wet years. Similarly, temperatures and PET anomalies below 50 % indicate cold years, while values above 50 % suggest warm years. To further distinguish severe drought (hot) from normal dry (hot) conditions, the 20th and 80th percentiles are employed to identify very dry (cool) and very wet (hot) conditions, respectively. The 20th and 80th percentiles are widely used in the literature for defining extreme conditions that have adverse impacts (Guntu et al., 2023; Mishra et al., 2020). Narrower thresholds like 10th and 90th percentiles might provide information in detecting very extreme condition. However, they also introduce noise (inter-annual disruption) into the investigation of the long-term development for the hydro-climatic processes. By applying these thresholds, the hydro-climatic time series are divided into four distinct categories of dry and wet (cool and hot) conditions: below 20 %, 20–50 %, 50–80 %, and above 80 %. Through the application of normalized percentile ranking analysis, we visually compare the various categories, thereby revealing the onset, intensity, and duration of hydro-climatic extremes,
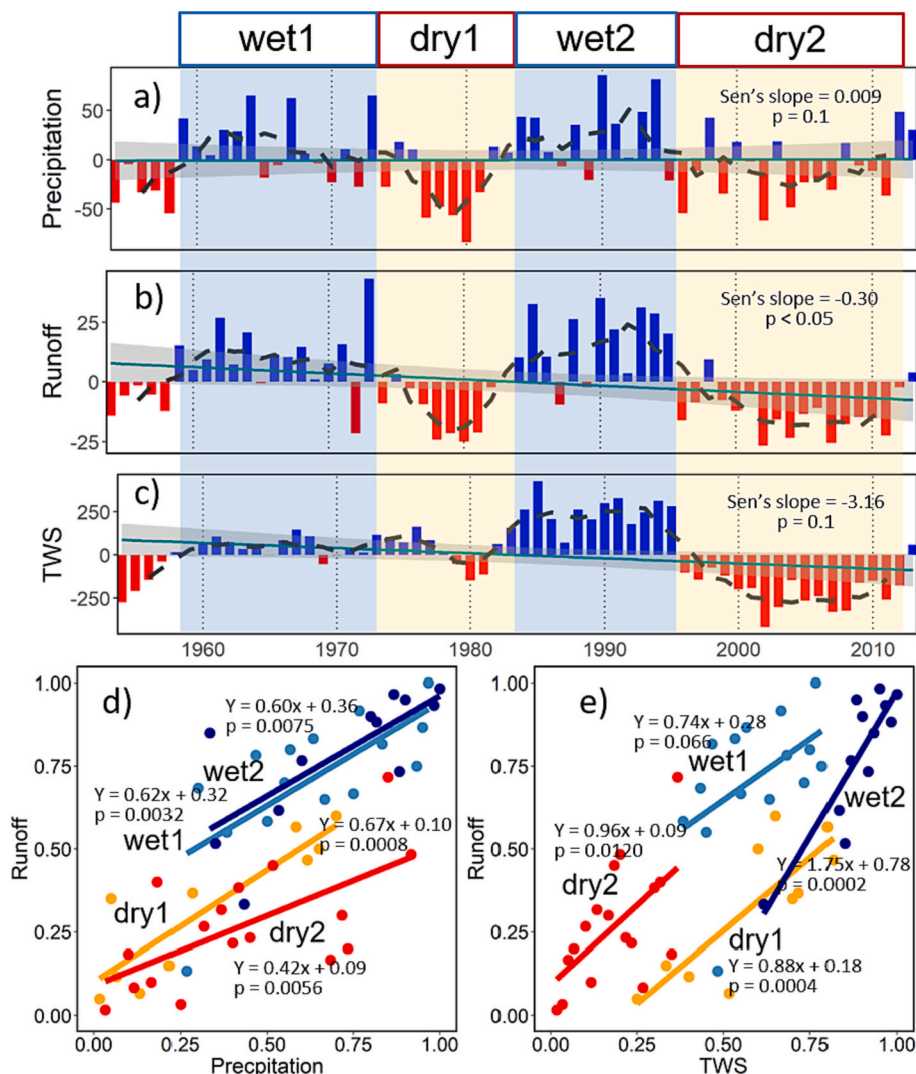
Table 1
Dataset details.

Data type	Data category	Dataset	Resolution	Frequency	Period	Data source
Permafrost data	Active layer thickness (ALT)	CALM	Point (Station)	Yearly	1996–2009	https://www2.gwu.edu/~calm/
Runoff data	Runoff (R)	GRDC	Point (Station)	Monthly	1954–2013	GRDC; http://www.bafg.de/GRDC/
Global gridded data	Air temperature (T) Potential evapotranspiration (PET)	CRU	0.5° × 0.5°	Monthly	1954–2013	Harris et al., 2014
	Precipitation (P)	GPCC	0.5° × 0.5°	Monthly	1954–2013	Schneider et al., 2018
	Reconstructed GRACE terrestrial water storage (TWS)	GRACE-REC	0.5° × 0.5°	Monthly	1954–2013	Humphrey and Gudmundsson, 2019
	Geopotential height patterns (850-hPa and 500-hPa)	NCEP/NCAR Reanalysis	2.5° × 2.5°	Monthly	1954–2013	Kalnay et al., 1996

Fig. 2. a-c show the anomalies of annual precipitation (mm), runoff (mm), and TWS (mm) relative to a long-term average over 1954–2013 in the Selenga basin. Solid lines represent the linear trends; grey shading indicates the 95 % confidence level; dashed black lines denote the 5-year moving averages. d) presents the runoff-precipitation regression; while e) shows the runoff-TWS regression. The light blue dots refer to wet1, the dark blue dots denote wet2, while the yellow and red dots represent dry1 and dry2, respectively.

which is particularly insightful for understanding the compound extremes. This systematic approach enables us to analyze the temporal progression and variations of these hydro-climate factors, providing a more informed comprehension of the intricate regime shifts in hydrology and climate over time.

4. Results

Large-scale permafrost degradation, induced by increased temperatures, has been observed in recent studies in the Selenga region (Ishikawa et al., 2018; Wu et al., 2022a, 2022b; Wang et al., 2022; Yamkhin et al., 2022; Walther and Kamp, 2023). Based on the 0 °C isotherm of mean annual air temperature (MAAT), we identify a discernible northward movement during the period 1984–2013 compared to the preceding 30 years (Fig. S4). This shift implies significant lateral permafrost degradation and potentially wholescale permafrost loss at the southern edge of the permafrost domain. The observed active layer thickness (ALT), based on 11 borehole stations from CALM networks during 1996–2009 in the Selenga region (Table S1), also shows a consistent increase across all monitored stations (Fig. S5), with the most significant thickness increase observed in station M1.A, ranging from 3.9 m to 8.2 m

over this period. Given that warming-induced permafrost degradation modifies the connections between surface and subsurface hydrological systems, one would expect that it also influences the land-hydrology-atmosphere couplings.

In the following, we examine the evidence of such consequences from comparative investigations of the dry conditions in the hydro-climatic variables during 1954–2013 across the semi-arid Selenga catchment. In Section 4.1, by comparing interannual variabilities of precipitation, runoff, and TWS with their long-term averages, we first identify two alternative dry and wet spells, respectively, in the hydrological dynamics. The decreasing trends in runoff and TWS, as well as the reduced runoff-generation efficiency, provide a first consequence of permafrost degradation. Subsequently, in Section 4.2, we analyze how such a consequence may have propagated into the atmospheric systems with an exacerbated hydrological drought in the second dry spell. The direct link between the permafrost degradations and drying condition is then investigated in Section 4.3 based on the long-term and periodic relationship between the Thawing Index (TI) and runoff deficits.

4.1. Characteristics of two dry spells and their implication on water availability

4.1.1. Intensified Hydrological Droughts with prolonged duration in dry2

Fig. 2 illustrates the historical anomalies of precipitation, river runoff, and terrestrial water storage (TWS), compared to their 60-year averages, respectively, spanning from 1954 to 2013. Despite an absence of an apparent trend in annual precipitation (0.009 mm/yr, $p =$ 0.9), significant long-term trends are observed in river runoff (-0.30 mm/yr, $p < 0.05$) and TWS (-3.16 mm/yr, $p = 0.1$). Considering the notable warming in the Selenga region (Fig. S 3), one might expect that the decreased runoff and TWS could be induced by increased evapotranspiration (ET). However, in our previous study (Han and Menzel, 2022), we found a slight reduction in actual ET during 1984–2013. These distinct trends among the hydrological components indicate a strong control of landscape properties on the hydrological response to climate forcing, further suggesting that an enhanced infiltration and percolation induced by permafrost degradation could be a major driver for the reduction in runoff and TWS. A more detailed discussion on the relationship between permafrost degradation and hydrological change is presented afterward in Section 4.4.

In addition to long-term trends, these three variables have exhibited alternative oscillations between wet and dry states, resulting in two well-defined wet and dry spells, denoted as wet1 (1958–1973, 16 yrs), dry1 (1974–1983, 10 yrs), wet2 (1984–1995, 12 yrs) and dry2 (1996–2012, 17 yrs), respectively. These four wet and dry spells are determined based on the anomalies of river discharge. For example, most of the year in the dry1 and dry2 show negative anomalies in runoff, and vice versa. The observed oscillation patterns are primarily influenced by the natural variability of the atmospheric circulation over the study region (Han and Menzel, 2022). It is noteworthy that the consistent results between precipitation, river runoff and TWS are remarkable. Especially, the TWS data utilized in this analysis is derived from 100 ensemble members generated by a learning-based model, rendering it an entirely distinct dataset from the records of precipitation and river runoff. This distinction further reinforces the significance of the consistent findings across these three independent datasets.

The focus of this research is to investigate the dry dynamics of the two dry spells, namely, dry1 and dry2 in this semi-arid Selenga catchment. During both dry1 and dry2 periods, water deficits begin with insufficient precipitation (precipitation deficits). These deficits then gradually propagate over months to years through the hydrological system, ultimately leading to reduced water availability, expressed by declining river runoff and TWS. However, distinct patterns are evident between dry1 and dry2 periods. While the precipitation deficits in dry2 are less intense compared to dry1, the dry conditions in river runoff and TWS during dry2 are more severe and longer lasting. For example, during the dry2 period, river discharge consistently remained below average from 1999 to 2012, even though there are individual wet annual precipitation years, such as in 1998, 2000, 2003, 2008, and 2012. This situation is further mirrored in TWS anomalies, which exhibit even more pronounced declines. Such a prolonged dry condition over multiple years has been documented in previous paleoclimatic investigations (Davi et al., 2010; Hessl et al., 2018). However, it is worth noting that its severity is uncommon within the documented instrumental hydro-climatic records (Zhang et al., 2020). While these dry spells are mainly driven by the climatic precipitation deficit, we expect that the permafrost-degradation related landscape changes shall also play an important role.

4.1.2. Decreased efficiency of runoff generation from precipitation

The role of permafrost degradation in modifying the drying dynamics is more evident in the runoff-generation efficiency shown in Fig. 2d and e. These figures are generated based on the normalized percentiles ranking series of the precipitation, runoff and TWS (see Section 3.2.2 for more details). With this, significant differences in the hydro-climatic relationships between dry and wet periods are observed. First of all, as shown in Fig. 2d, though there is a consistent statistical relationship between precipitation and runoff during the two wet periods, the runoff-generation efficiency from precipitation during the dry periods was considerably lower compared to that of wet periods. These results indicate that, owing to the increased atmospheric water demand during dry periods, the hydrological system requires a higher amount of water from precipitation to maintain surface water availability. This manifests as reduced efficiency in converting precipitation into river runoff during dry spells. Such situation is even more pronounced during the dry2 period from 1996 to 2012, as indicated by a relatively flat regression line between runoff and precipitation. Considering the significant warming condition during last decades (Fig. S 3) and decreasing actual ET (Han and Menzel, 2022), this reduction in generated runoff efficiency from precipitation might be potentially induced by the permafrost degradation induced enhancement in infiltration and percolation.

Fig. 2e presents the comparison between TWS and runoff. Notably, the runoff patterns in both dry2 and wet2 exhibits higher dependence on TWS compared to the patterns observed in dry1 and wet1. This suggests an intensified surface-subsurface water connection during the warming periods in wet2 and dry2, contrasting with the earlier dry and wet periods. This enhanced connectivity in surface-subsurface water system is another evidence of potential consequence of lateral degradation of permafrost (Walvoord and Kurylyk, 2016).

4.2. Co-occurred land-atmospheric warming and drying conditions

4.2.1. Drying with intensified warming during dry2

Before addressing how permafrost degradation may affect the dry conditions in the semi-arid Selenga region in a coupled land-atmospheric perspective, we first analyze how other climatic variables namely, temperature and PET, are related to the hydrological drying conditions. Demonstrated via percentiles analysis shown in Fig. 3, the prolonged hydrological drought spanning from 1996 to 2012 (i.e. dry2) coincides with notable positive anomalies in both air temperature and PET. This intriguing phenomenon of concurrent warm and dry conditions is particularly pronounced during summer (June–August, as depicted in the lower panel of Fig. 3. It is worth noting that during this period, precipitation and temperature exhibited a highly coupled relationship within the atmospheric system.

These concurrent phenomena indicate enhanced land-atmospheric interactions within the hydro-climate system, potentially leading to increased actual evapotranspiration (ET). However, as mentioned in Section 4.1, our prior investigation revealed a reduction in actual evapotranspiration during the period 1984–2013 in the Selenga catchment (Han and Menzel, 2022, Fig. 3). This suggests an insufficient water supply from the dry land surface to meet the heightened atmospheric water demand in the region. Consequently, this discrepancy exacerbates the atmospheric moisture deficiency, leading to an increase in vapor pressure deficit. This, in turn, triggers increased potential evapotranspiration (PET) and higher portion of available energy through sensible heat flux, further warming the already dry surface. The intensified coupling between land, hydrology, and atmosphere is also evident by the simultaneous occurrence of positive anomalies in potential evapotranspiration (PET) and water deficits in hydrological variables (Fig. S 3 in the Supplement). The resulting drying hydro-climate system in the Selenga region may also be exacerbated by the dry impact of lateral permafrost degradation (Ford and Frauenfeld, 2016; Han and Menzel, 2022), and will be discussed later.

4.2.2. Enhanced summer atmospheric dynamics in Mongolia

In perspective of a coupled hydro-climatic system, the occurrence of joint hot-dry conditions is strongly evidenced from the enhanced land-atmosphere coupling with a heightened blocking pattern in atmospheric conditions (Miralles et al., 2019). In other words, the extremely
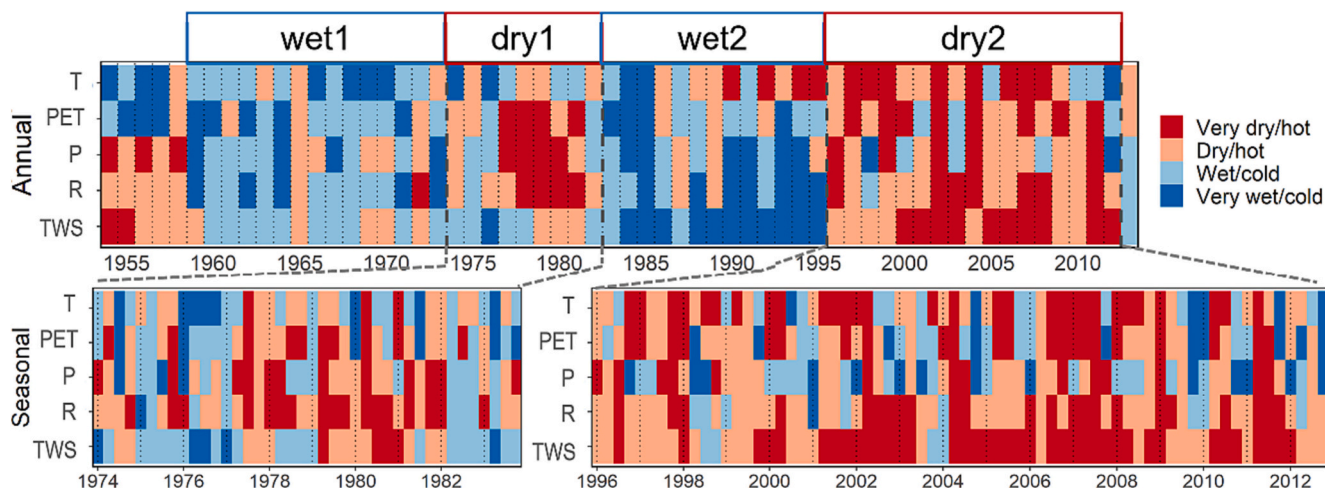
Fig. 3. Dry and wet spells based on the percentile ranking analysis during the period of 1954–2013. The upper and lower panels display the annual and seasonal categories of the hydro-climate variables (T, PET, P, R and TWS). The upper panel presents the four dry and wet periods based on the annual conditions. Since this study mainly focuses on the two dry periods (dry1 and dry2), the enlarged properties of dry1 and dry2 for each season are displayed in the lower panel.

dry land surface can reinforce high temperatures and reduce moisture availability in the atmosphere, and thus can contribute to the development of an intensified high-pressure system in the atmosphere.

To investigate this further, we analyzed the patterns of 500-hPa and 850-hPa geopotential height during the two dry periods by comparing them to the long-term condition from 1954 to 2013 (Fig. 4). Our findings reveal that the second dry period from 1996 to 2012 experienced an amplification of positive geopotential height anomalies in both 500-hPa (Z500) and 850-hPa (Z850) specifically over the Selenga River catchment, in contrast with the rest of the region in Siberia. This amplification indicates high-pressure blocking patterns in the middle and lower levels of the atmosphere (Z500, Z850) over the Mongolian Plateau, which restrict moisture supply to the Selenga catchment, ultimately leading to reduced precipitation. Additionally, the positive anomalies in Z500 and
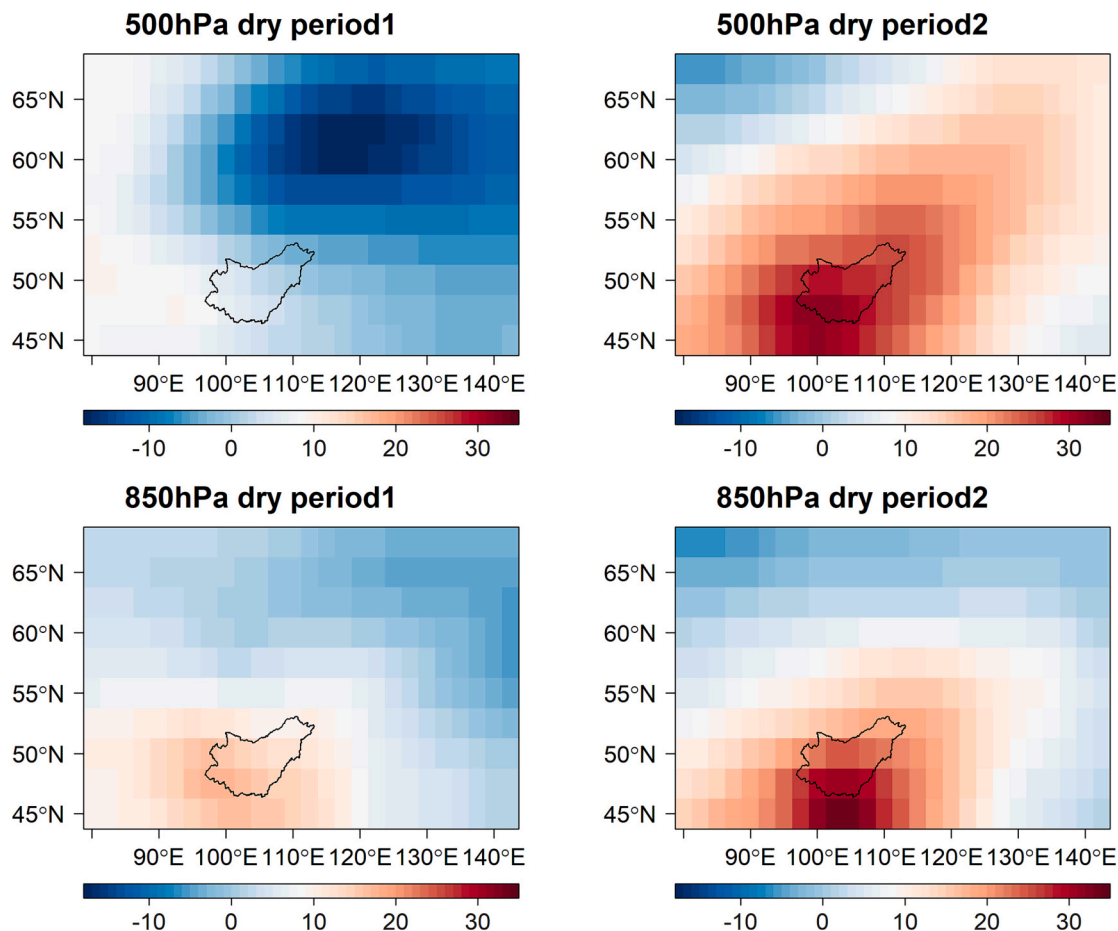

Fig. 4. Geopotential height anomalies (gpm) at 500 hPa and 850 hPa during two dry periods: dry period1 (1974–1983) and dry period2 (1996–2012) relative to the reference period from 1954 to 2013.

Z850 could dynamically induce clear sky, a warm atmosphere, and prolonged hot conditions on the land. This combination of land-atmospheric factors can contribute to the development of severe heat-waves on the land surface, as supported by previous research (Meehl and Tebaldi, 2004; Sato and Nakamura, 2019).

However, during the first dry period (1974–1983, dry1), which was also characterized by deficit moisture conditions, there were no such enhanced blockings in the geopotential height as that observed during dry2. This implies that the occurrence of enhanced land-atmosphere coupling, which could lead to an intensified drying condition, might not have been present during the first dry period. This observation strongly indicates that there is a significant change in the highly coupled land-hydrology-atmosphere system under rapid warming conditions during the more recent dry period (dry2). Again, considering the widespread presence of permafrost in the Selenga catchment, we expect such a change might be another evidence for the role of (lateral) permafrost degradation in intensifying the drying conditions in semi-arid cold regions.

4.3. Relationship between warming permafrost and runoff deficits

We further employ the anomalies of Thawing Index (TI) to represent the long-term change of permafrost thermal condition. Fig. 5 illustrates the long-term evolution of TI anomalies as compared to the reference period 1954–2013 in the Selenga catchment. Similar to the long-term warming trend detected from air temperature, TI resembles a consistent upward trend (4.8 °C-days/yr, $p < 0.001$) during the period 1954–2013. Notably, a distinct shift in TI becomes apparent after 1996, with all yearly anomalies demonstrating positive values. This clear shift pattern in TI together with the increased ALT reflect the permafrost degradation in the Selenga catchment, which align cohesively with water deficits in hydro-climatic variables from 1996 to 2012, suggesting a potential connection between permafrost degradation and drying conditions.

To validate this hypothesis that there might be a connection between permafrost degradation and drying conditions, we analyzed the regression between TI anomalies and runoff deficits across distinct dry and wet periods during 1954–2013 in the Selenga catchment (Fig. 6). Generally, a consistent negative relationship is observed between TI and runoff deficits, suggesting that thawing permafrost may exacerbate the deficits in river runoff. This relationship arises due to the potential intensification of connections between surface and subsurface hydrological systems under thawing permafrost conditions, which triggers downward soil moisture movement. Consequently, enhanced infiltration resulting from permafrost degradation could lead to a reduction in surface runoff. This effect is particularly pronounced during the prolonged second dry spell spanning from 1996 to 2012. Furthermore, this period exhibited concurrent runoff deficits and heightened positive TI values, indicating that permafrost degradation during this warm decade
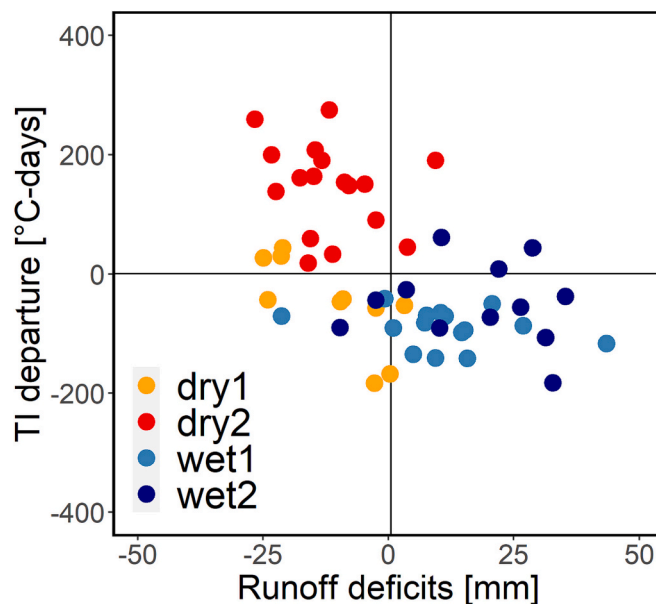

Fig. 6. Regression of anomalies for Thawing Index (TI) and runoff deficits during each dry and wet period. TI serves as an indicator of permafrost condition, with higher values referring to intensified thawing. Runoff deficits and positive TI co-occurred during 1996–2012 (dry2), suggesting enhanced drying conditions triggered by warming (i.e., degrading) permafrost.

further reinforces water scarcity in the Selenga area.

5. Discussion

Through comprehensive investigations, we demonstrated how large-scale lateral permafrost degradation might exacerbate drying conditions in terms of reducing surface water storage and amplifying warming condition in low-level atmosphere. This represents an extension of previous hydrological studies on permafrost degradation-induced drying consequences (Jones et al., 2022; Haynes et al., 2018; Boike et al., 2016; Carroll et al., 2011; Smith et al., 2005) by including the interaction with atmosphere. We expect that such coupled land (permafrost)-hydrological-atmospheric investigation provides an explanation of the intensified drying and warming condition in the northern Mongolian Plateau in recent decades found in tree-ring based studies (Pederson et al., 2014; Hessl et al., 2018; Zhang et al., 2020). In the following, we first expand the discussion on how permafrost degradation intensifies drying and warming in land-atmosphere system, and its implications to the semi-arid Selenga region. Then we will also discuss the validity of TI in detecting long-term evolution of permafrost at large spatial scale.
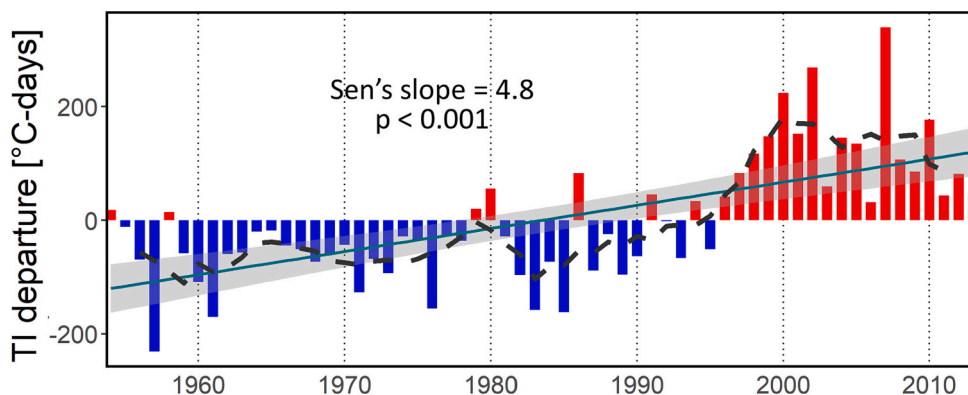

Fig. 5. Inter-annual variability of Thawing Index (TI) anomalies during 1954–2013 in the Selenga catchment.

5.1. Permafrost degradation intensifies dry and hot land-atmosphere system

Multiple drivers within the land-atmosphere system and their complex interactions could yield below-normal water conditions in the hydrological variables (Fu et al., 2007; Van Loon, 2015; Miralles et al., 2019). Driven by quasi-stationary atmospheric oscillations, the terrestrial water availability in the Selenga River basin exhibits two distinctive dry spells: 1974–1982 and 1996–2012, respectively. The second dry spell (1996–2012) surpasses the preceding period (1974–1982) both in terms of duration and magnitude of moisture deficits observed in river runoff and total water storage (TWS), relative to the precipitation difference (Fig. 2). This disproportional hydro-climate response in dry2 indicates that the hydrological drought in the Selenga region is not only controlled by the precipitation deficiencies, but also significantly depends on the storage and exchange of the water fluxes between the surface and subsurface hydrological system (Van Loon, 2015), which might be modified by permafrost degradation: as the climate warms, an increased extent of permafrost-free areas in the Selenga region may trigger more water infiltration and percolation into the subsurface system, and a drier surface condition (Ishikawa et al., 2005; Ford and Frauenfeld, 2016). The robust negative relationship between TI and runoff deficits (Fig. 6) provides direct evidence for a potential linkage between permafrost degradation and hydrological droughts.

In turn, the water deficits induced by lateral permafrost degradation in land surface could lead to higher sensible heat in comparison to latent heat, inducing higher temperature and intensified moisture deficiency (i.e., increasing vapor pressure deficit) in the atmosphere. Meanwhile, this process is accompanied by more frequent clear sky and low precipitation, eventually resulting in drier state in land-surface. This exacerbated dry and hot condition is evident from our investigation on the coincidence of water deficits in hydrological system with positive anomalies in air temperature and potential evapotranspiration, as well as low-level geopotential in Fig. 3–4. These observed concurrent "hot-dry" conditions in hydro-climate variables, aligning with intensified anticyclonic patterns at lower levels of the atmosphere, further indicate a robust strengthening of land-atmosphere interactions, as indicated by previous studies (Zscheischler et al., 2020; Seneviratne et al., 2006; Zhang et al., 2020; Meehl and Tebaldi, 2004; Diffenbaugh et al., 2015; Martin et al., 2020). The simultaneous presence of severe water deficits, elevated air temperature, and enhanced permafrost degradation imply that, in a warmer climate, precipitation deficit is more prone to yield consecutive drying conditions in semi-arid cold region. Such compound extreme events underscore the growing significance of warming climate as a critical trigger for the drought risk in permafrost-affected area.

5.2. Consequence of intensified land-atmospheric coupling in the Selenga region

Selenga is a vital transboundary river connecting Mongolia and Russia, and it also stands as a principal tributary of Lake Baikal. The increasing water demand from ecological systems and human consumption is expected to strain the already restricted water supply in this semi-arid region (Priess et al., 2011; Van Loon, 2015). Therefore, the drought detected in our study could further escalate the tension in water deficits. Particularly, our findings highlight a notable decline in runoff efficiencies since the mid-1990s across the Selenga River basin. Together with the enhanced effects of warming, including heightened atmospheric moisture and enhanced permafrost degradation, it might lead to an irreversible regime shift in the hydro-climatic system in the transition region.

The severity of these acute water shortages could disrupt daily life, socio-economic structures, ecological well-being, and potentially strain the water resource management cooperation between upstream Mongolia and downstream Russia (Karthe et al., 2017). Through a comprehensive investigation of shifts in water availability in the context

of a changing climate and thawing permafrost, this study provides essential insights for water resource managers and policymakers. These insights could potentially facilitate the development of a comprehensive water-sharing agreement that effectively balances the competing water demands, thereby mitigating potential conflicts. Ultimately, these efforts could contribute to reducing the vulnerability of this transitional region to potential water scarcity as the climate continues to warm.

5.3. Detecting long-term permafrost degradation

We note that, due to monitoring difficulties in cold remote regions, the Selenga catchment suffers from scarce permafrost observation data. Direct permafrost observations span only recent decades (starting from the 1990s) through the Circumpolar Active Layer Monitoring (CALM) Program Network (Brown et al., 2000). Therefore, quantifying the long-term evolution of permafrost remains a critical challenge (Walvoord and Kurylyk, 2016).

Various approaches have been proposed to address the above issue (Walvoord and Kurylyk, 2016). In one approach, numerical modeling has been employed to simulate permafrost thawing and freezing processes (Frampton et al., 2011; Gouttevin et al., 2012; Y. Zhang et al., 2013), representing complex dynamics of water and heat in the subsurface (Walvoord and Kurylyk, 2016). However, achieving optimal model performance needs a vast of physical parameters which are typically uncertain due to limited field observations (Riseborough et al., 2008), and the accuracy of model performance (especially for large catchments) is consequently debated (Kurylyk et al., 2014). Another method to reflect the historical evolution of permafrost utilizes long-term river base flow records sustained by groundwater (Brutsaert and Hiyama, 2012; S. Lyon et al., 2009; S. W. Lyon and Destouni, 2010). While it is widely applied in permafrost detection across regions such as Siberia (Brutsaert and Hiyama, 2012), North America (S. W. Lyon and Destouni, 2010), and Scandinavia (S. Lyon et al., 2009), this approach strongly relies on daily streamflow data, often plagued by high uncertainties and scarce availabilities in cold regions (Shiklomanov et al., 2006).

To detect the long-term large-scale evolution of permafrost, our study uses TI to represent permafrost degradation (Frauenfeld and Zhang, 2011; Frauenfeld et al., 2007; Peng et al., 2018). Since the air temperature (CRU) data is available at long-term and global scale, this method provides a first-order estimation of the basin-wide permafrost evolution during 1954–2013. In previous study, TI has been employed to reflect the warming conditions in permafrost across the Northern Hemisphere (Frauenfeld et al., 2007; Peng et al., 2018), the Russian Arctic catchments (Wang et al., 2022), as well as Qinghai-Tibet Plateau (Wu et al., 2013). The application of this method is plausible, as demonstrated by previous studies showing a correlation between observed warming permafrost trend and rising air temperature (Biskaborn et al., 2019; Smith et al., 2022), though local land properties, such as topography, snow cover, and vegetation, could also impact permafrost response to a warming climate (Jorgenson et al., 2010).

6. Conclusions

In this study, we demonstrate that permafrost degradation can have significant impact on the drought dynamics in the semi-arid Selenga River basin. This is obtained based on comparative investigations of the two historical dry spells with distinct permafrost conditions, i.e., 1974–1983 and 1996–2012. Initially, changes in atmospheric circulation has led to long-lasting precipitation deficiencies during 1996–2012. Subsequently, the degradation of permafrost enhances infiltration and percolation in the hydrological system, leading to more reduction in runoff and terrestrial water storage (TWS). As a consequence, the water deficits in runoff and terrestrial water storage (TWS) during the second dry spell are more vigorous in intensity than that in the first dry spell. Meanwhile, the runoff generation becomes more dependent on TWS

than on precipitation, implying potential development of groundwater-dominated hydrological system in the sensitive permafrost boundary region. Moreover, permafrost degradation also exacerbates the concurrent presence of hot and dry conditions within the hydro-climate system, resulting in an intensified anticyclonic atmospheric pattern. These compounding patterns suggest an enhanced coupling between the land and atmosphere in the semi-arid Selenga region, which may elevate local temperature and in turn accelerate permafrost degradation. What is worse, the enhanced land-atmosphere coupling might also alter the drought dynamics that could potentially reinforce the water scarcity. This could eventually trigger an irreversible shift in the availability of water resources. Our findings could benefit regional water resource management, human health, and ecosystem function in semi-arid permafrost region.

CRediT authorship contribution statement

Li Han: Conceptualization, Data curation, Formal analysis, Investigation, Methodology, Resources, Validation, Visualization, Writing – original draft, Writing – review & editing. **Lucas Menzel:** Conceptualization, Methodology, Supervision, Writing – review & editing.

Declaration of competing interest

The authors declare that they have no known competing financial interests or personal relationships that could have appeared to influence the work reported in this paper.

Data availability

Data will be made available on request.

Acknowledgements

References

Bagley, J.E., Desai, A.R., Harding, K.J., Snyder, P.K., Foley, J.A., 2014. Drought and deforestation: has land cover change influenced recent precipitation extremes in the Amazon? J. Clim. 27 (1), 345–361.

Batima, P., Natsagdorj, L., Gombluudev, P., Erdenetsetseg, B., 2005. Observed climate change in Mongolia. Assess Imp. Adapt. Clim. Change Work Pap. 12, 1–26.

Biskaborn, B.K., Smith, S.L., Noetzli, J., Matthes, H., Vieira, G., Streletskiy, D.A., Lantuit, H., 2019. Permafrost is warming at a global scale. Nat. Commun. 10 (1), 1–11.

Boike, J., Grau, T., Heim, B., Günther, F., Langer, M., Muster, S., Lange, S., 2016. Satellite-derived changes in the permafrost landscape of central Yakutia, 2000–2011: wetting, drying, and fires. Glob. Planet. Chang. 139, 116–127.

Brown, J., Hinkel, K.M., Nelson, F.E., 2000. The circumpolar active layer monitoring (CALM) program: research designs and initial results. Polar Geogr. 24 (3), 166–258.

Brutsaert, W., Hiyama, T., 2012. The determination of permafrost thawing trends from long-term streamflow measurements with an application in eastern Siberia. J. Geophys. Res. Atmos. 117 (D22).

Carroll, M.L., Townshend, J.R.G., DiMiceli, C.M., Loboda, T., Sohlberg, R.A., 2011. Shrinking lakes of the Arctic: spatial relationships and trajectory of change. Geophys. Res. Lett. 38 (20).

Chalov, R., s. Jarsjö, J., Kasimov .O., N.S., Romanchenko, A., Pietroń, J., Thorslund, J., Promakhova, E.V., 2015. Spatio-temporal variation of sediment transport in the Selenga River Basin, Mongolia and Russia. Environ. Earth Sci. 73, 663–680.

Cook, B.I., Miller, R.L., Seager, R., 2009. Amplification of the North American "Dust Bowl" drought through human-induced land degradation. Proc. Natl. Acad. Sci. 106 (13), 4997–5001.

Cook, B.I., Mankin, J.S., Anchukaitis, K.J., 2018. Climate change and drought: from past to future. Curr. Clim. Chang. Rep. 4 (2), 164–179.

Davi, N., Jacoby, G., Fang, K., Li, J., D'Arrigo, R., Baatarbileg, N., Robinson, D., 2010. Reconstructing drought variability for Mongolia based on a large-scale tree ring network: 1520–1993. J. Geophys. Res. Atmos. 115 (D22).

Diffenbaugh, N.S., Swain, D.L., Touma, D., 2015. Anthropogenic warming has increased drought risk in California. Proc. Natl. Acad. Sci. 112 (13), 3931–3936.

Dobinski, W., 2011. Permafrost. Earth Sci. Rev. 108 (3–4), 158–169.

Ford, T.W., Frauenfeld, O.W., 2016. Surface–atmosphere moisture interactions in the frozen ground regions of eurasia. Sci. Rep. 6 (1), 1–9.

Frampton, A., Painter, S., Lyon, S.W., Destouni, G., 2011. Non-isothermal, three-phase simulations of near-surface flows in a model permafrost system under seasonal variability and climate change. J. Hydrol. 403 (3–4), 352–359.

Frauenfeld, O.W., Zhang, T., 2011. An observational 71-year history of seasonally frozen ground changes in the Eurasian high latitudes. Environ. Res. Lett. 6 (4), 044024.

Frauenfeld, O.W., Zhang, T., Mccreight, J.L., 2007. Northern hemisphere freezing/thawing index variations over the twentieth century. Int. J. Climatol. 27 (1), 47–63.

Frolova, N.L., Belyakova, P.A., Grigor'ev, V.Y., Sazonov, A.A., Zotov, L.V., 2017. Many-year variations of river runoff in the Selenga basin. Water Res. 44, 359–371.

Fu, G., Charles, S.P., Chiew, F.H.S., 2007. A two-parameter climate elasticity of streamflow index to assess climate change effects on annual streamflow. Water Resour. Res. 43 (11).

Gouttevin, I., Krinner, G., Ciais, P., Polcher, J., Legout, C., 2012. Multi-scale validation of a new soil freezing scheme for a land-surface model with physically based hydrology. Cryosphere 6 (2), 407–430.

Gruber, S., 2012. Derivation and analysis of a high-resolution estimate of global permafrost zonation. Cryosphere 6 (1), 221–233.

Guntu, R.K., Merz, B., Agarwal, A., 2023. Increased likelihood of compound dry and hot extremes in India. Atmos. Res. 290, 106789.

Han, L., Menzel, L., 2022. Hydrological variability in southern Siberia and the role of permafrost degradation. J. Hydrol. 604, 127203.

Harris, I.P.D.J., Jones, P.D., Osborn, T.J., Lister, D.H., 2014. Updated high-resolution grids of monthly climatic observations–the CRU TS3. 10 Dataset. Int. J. Climatol. 34 (3), 623–642.

Haynes, K.M., Connon, R.F., Quinton, W.L., 2018. Permafrost thaw induced drying of wetlands at Scotty Creek, NWT, Canada. Environ. Res. Lett. 13 (11), 114001.

Hermans, K., McLeman, R., 2021. Climate change, drought, land degradation and migration: exploring the linkages. Curr. Opin. Environ. Sustain. 50, 236–244.

Hessl, A.E., Anchukaitis, K.J., Jelsema, C., Cook, B., Byambasuren, O., Leland, C., Hayles, L.A., 2018. Past and future drought in Mongolia. Sci. Adv. 4 (3), e1701832.

Humphrey, V., Gudmundsson, L., 2019. GRACE-REC: a reconstruction of climate-driven water storage changes over the last century. Earth Syst. Sci. Data 11 (3), 1153–1170.

Ishikawa, M., Sharkhuu, N., Zhang, Y., Kadota, T., Ohata, T., 2005. Ground thermal and moisture conditions at the southern boundary of discontinuous permafrost, Mongolia. Permafr. Periglac. Process. 16 (2), 209–216.

Iijima, Y., Ohta, T., Kotani, A., Fedorov, A.N., Kodama, Y., Maximov, T.C., 2014. Sap flow changes in relation to permafrost degradation under increasing precipitation in an eastern siberian larch forest. Ecohydrology 7 (2), 177–187.

Ishikawa, M., Jamvaljav, Y., Dashtseren, A., Sharkhuu, N., Davaa, G., Iijima, Y., Yoshikawa, K., 2018. Thermal states, responsiveness and degradation of marginal permafrost in Mongolia. Permafr. Periglac. Process. 29 (4), 271–282.

Jones, B.M., Grosse, G., Farquharson, L.M., Roy-Léveillée, P., Veremeeva, A., Kanevskiy, M.Z., Hinkel, K.M., 2022. Lake and drained lake basin systems in lowland permafrost regions. Nat. Rev. Earth Environ. 3 (1), 85–98.

Jorgenson, M.T., Romanovsky, V., Harden, J., Shur, Y., O'Donnell, J., Schuur, E.A., Marchenko, S., 2010. Resilience and vulnerability of permafrost to climate change. Can. J. For. Res. 40 (7), 1219–1236.

Jung, M., Reichstein, M., Ciais, P., Seneviratne, S.I., Sheffield, J., Goulden, M.L., Zhang, K., 2010. Recent decline in the global land evapotranspiration trend due to limited moisture supply. Nature 467 (7318), 951–954.

Kalnay, E., Kanamitsu, M., Kistler, R., Collins, W., Deaven, D., Gandin, L., Joseph, D., 1996. The NCEP/NCAR 40-year reanalysis project. Bull. Am. Meteorol. Soc. 77 (3), 437–472.

Karthe, D., Chalov, S., Moreido, V., Pashkina, M., Romanchenko, A., Batbayar, G., Flörke, M., 2017. Assessment of runoff, water and sediment quality in the Selenga River basin aided by a web-based geoservice. Water Res. 44 (3), 399–416.

Kasimov, N., Shinkareva, G., Lychagin, M., Kosheleva, N., Chalov, S., Pashkina, M., Jarsjö, J., 2020. River water quality of the Selenga-Baikal Basin: part I—Spatio-temporal patterns of dissolved and suspended METls. Water 12 (8), 2137.

Klinge, M., Dulamsuren, C., Erasmi, S., Karger, D.N., Hauck, M., 2018. Climate effects on vegetation vitality at the treeline of boreal forests of Mongolia. Biogeosciences 15 (5), 1319–1333.

Kopp, B.J., Minderlein, S., Menzel, L., 2014. Soil moisture dynamics in a mountainous headwater area in the discontinuous permafrost zone of northern Mongolia. Arct. Antarct. Alp. Res. 46 (2), 459–470.

Kurylyk, B.L., MacQuarrie, K.T., McKenzie, J.M., 2014. Climate change impacts on groundwater and soil temperatures in cold and temperate regions: Implications, mathematical theory, and emerging simulation tools. Earth Sci. Rev. 138, 313–334.

Lu, C., Tian, H., Zhang, J., Yu, Z., Pan, S., Dangal, S., Hessl, A., 2019. Severe long-lasting drought accelerated carbon depletion in the Mongolian Plateau. Geophys. Res. Lett. 46 (10), 5303–5312.

Lyon, S.W., Destouni, G., 2010. Changes in catchment-scale recession flow properties in response to permafrost thawing in the Yukon river basin. Int. J. Climatol. 30 (14), 2138–2145.

Lyon, S., Destouni, G., Giesler, R., Humborg, C., Mörth, M., Seibert, J., Troch, P., 2009. Estimation of permafrost thawing rates in a sub-arctic catchment using recession flow analysis. Hydrol. Earth Syst. Sci. 13 (5), 595–604.

Mariano, D.A., dos Santos, C.A., Wardlow, B.D., Anderson, M.C., Schiltmeyer, A.V., Tadesse, T., Svoboda, M.D., 2018. Use of remote sensing indicators to assess effects of drought and human-induced land degradation on ecosystem health in Northeastern Brazil. Remote Sens. Environ. 213, 129–143.

Martin, J.T., Pederson, G.T., Woodhouse, C.A., Cook, E.R., McCabe, G.J., Anchukaitis, K. J., King, J., 2020. Increased drought severity tracks warming in the United States' largest river basin. Proc. Natl. Acad. Sci. 117 (21), 11328–11336.

Meehl, G.A., Tebaldi, C., 2004. More intense, more frequent, and longer lasting heat waves in the 21st century. Science 305 (5686), 994–997.

Miralles, D.G., Gentine, P., Seneviratne, S.I., Teuling, A.J., 2019. Land–atmospheric feedbacks during droughts and heatwaves: state of the science and current challenges. Ann. N. Y. Acad. Sci. 1436 (1), 19–35.

Mishra, V., Thirumalai, K., Singh, D., Aadhar, S., 2020. Future exacerbation of hot and dry summer monsoon extremes in India. Npj Clim. Atmos. Sci. 3 (1), 10.

Munkhjargal, M., Yadamsuren, G., Yamkhin, J., Menzel, L., 2020. Ground surface temperature variability and permafrost distribution over mountainous terrain in northern Mongolia. Arct. Antarct. Alp. Res. 52 (1), 13–26.

Nelson, F.E., Outcalt, S.I., 1987. A computational method for prediction and regionalization of permafrost. Arct. Alp. Res. 19 (3), 279–288.

Obu, J., Westermann, S., Bartsch, A., Berdnikov, N., Christiansen, H.H., Dashtseren, A., Zou, D., 2019. Northern Hemisphere permafrost map based on TTOP modelling for 2000–2016 at 1 km2 scale. Earth Sci. Rev. 193, 299–316.

Pederson, N., Hessl, A.E., Baatarbileg, N., Anchukaitis, K.J., Di Cosmo, N., 2014. Pluvials, droughts, the Mongol Empire, and modern Mongolia. Proc. Natl. Acad. Sci. 111 (12), 4375–4379.

Peng, X., Zhang, T., Frauenfeld, O.W., Wang, K., Luo, D., Cao, B., Wu, Q., 2018. Spatiotemporal changes in active layer thickness under contemporary and projected climate in the Northern Hemisphere. J. Clim. 31 (1), 251–266.

Priess, J.A., Schweitzer, C., Wimmer, F., Batkhishig, O., Mimler, M., 2011. The consequences of land-use change and water demands in Central Mongolia. Land Use Policy 28 (1), 4–10.

Priess, J.A., Schweitzer, C., Batkhishig, O., Koschitzki, T., Wurbs, D., 2015. Impacts of agricultural land-use dynamics on erosion risks and options for land and water management in Northern Mongolia. Environ. Earth Sci. 73, 697–708.

Rao, M.P., Davi, N.K., D'Arrigo, R., D., Skees, J., Nachin, B., Leland, C., Byambasuren, O., 2015. Dzuds, droughts, and livestock mortality in Mongolia. Environ. Res. Lett. 10, 074012.

Rawlins, M.A., Steele, M., Holland, M.M., Adam, J.C., Cherry, J.E., Francis, J.A., Zhang, T., 2010. Analysis of the Arctic system for freshwater cycle intensification: observations and expectations. J. Clim. 23, 5715–5737.

Riseborough, D., Shiklomanov, N., Etzelmüller, B., Gruber, S., Marchenko, S., 2008. Recent advances in permafrost modelling. Permafr. Periglac. Process. 19 (2), 137–156.

Romanovsky, V.E., Smith, S.L., Christiansen, H.H., 2010. Permafrost thermal state in the polar Northern Hemisphere during the international polar year 2007–2009: a synthesis. Permafr. Periglac. Process. 21 (2), 106–116.

Sato, T., Nakamura, T., 2019. Intensification of hot Eurasian summers by climate change and land–atmosphere interactions. Sci. Rep. 9 (1), 1–8.

Schneider, U., Becker, A., Finger, P., Meyer-Christoffer, A., Ziese, M., 2018. GPCC full data monthly product at 0.58: Monthly land-surface precipitation from rain-gauges built on GTS-based and historical data, version 2018, 13. Deutscher Wetterdienst.

Seneviratne, S.I., Lüthi, D., Litschi, M., Schär, C., 2006. Land–atmosphere coupling and climate change in Europe. Nature 443 (7108), 205–209.

Seneviratne, S.I., Corti, T., Davin, E.L., Hirschi, M., Jaeger, E.B., Lehner, I., Teuling, A.J., 2010. Investigating soil moisture–climate interactions in a changing climate: a review. Earth Sci. Rev. 99, 125–161.

Shiklomanov, A.I., Yakovleva, T.I., Lammers, R.B., Karasev, I.P., Vörösmarty, C.J., Linder, E., 2006. Cold region river discharge uncertainty-estimates from large russian rivers. J. Hydrol. 326 (1–4), 231–256.

Slater, L.J., Anderson, B., Buechel, M., Dadson, S., Han, S., Harrigan, S., Wilby, R.L., 2021. Nonstationary weather and water extremes: a review of methods for their detection, attribution, and management. Hydrol. Earth Syst. Sci. 25 (7), 3897–3935.

Smith, S.L., Burgess, M.M., Riseborough, D., Mark Nixon, F., 2005. Recent trends from Canadian permafrost thermal monitoring network sites. Permafr. Periglac. Process. 16 (1), 19–30.

Smith, S.L., O'Neill, H.B., Isaksen, K., Noetzli, J., Romanovsky, V.E., 2022. The changing thermal state of permafrost. Nat. Rev. Earth Environ. 3 (1), 10–23.

Stefan, J., 1891. Über die Theorie der Eisbildung, insbesondere über die Eisbildung im Polarmeere. Ann. Phys. 278 (2), 269–286.

Tijdeman, E., Stahl, K., Tallaksen, L.M., 2020. Drought characteristics derived based on the Standardized Streamflow Index: a large sample comparison for parametric and nonparametric methods. Water Resour. Res. 56 (10), e2019WR026315.

Törnqvist, R., Jarsjö, J., Pietroń, J., Bring, A., Rogberg, P., Asokan, S.M., Destouni, G., 2014. Evolution of the hydro-climate system in the Lake Baikal basin. J. Hydrol. 519, 1953–1962.

Törnros, T., Menzel, L., 2010. Heading for knowledge in a data scarce river basin: Kharaa, Mongolia. In: Herrmann, A., Schumann, S. (Eds.), Status and Perspectives of Hydrology in Small Basins. IAHS Publication 336, Wallingford, pp. 270–275.

Trenberth, K.E., Dai, A., Van Der Schrier, G., Jones, P.D., Barichivich, J., Briffa, K.R., Sheffield, J., 2014. Global warming and changes in drought. Nat. Clim. Chang. 4 (1), 17–22.

United Nations Development Programme (UNDP), 2013. Chapter I. General characteristics of Lake Baikal Basin. In: State of the Environment Report. The Lake Baikal Basin 2012–2013; United Nations Development Programme: New York, NY, USA.

Van Loon, A.F., 2015. Hydrological drought explained. Wiley Interdiscip. Rev. Water 2 (4), 359–392.

Walther, M., Kamp, U., 2023. Mountain permafrost: a reflection on the periglacial environment in Mongolia. Geosciences 13 (9), 274.

Walvoord, M.A., Kurylyk, B.L., 2016. Hydrologic impacts of thawing permafrost—a review. Vadose Zone J. 15 (6).

Wang, Q., Okadera, T., Watanabe, M., Wu, T., Ochirbat, B., 2022. Ground warming and permafrost degradation in various terrestrial ecosystems in northcentral Mongolia. Permafr. Periglac. Process. 33 (4), 406–424.

Woo, M.K., 2012. Permafrost Hydrology. Springer Science & Business Media.

Wu, T., Wang, D., Mu, C., Zhang, W., Zhu, X., Zhao, L., Wu, X., 2022a. Storage, patterns, and environmental controls of soil organic carbon stocks in the permafrost regions of the Northern Hemisphere. Sci. Total Environ. 828, 154464.

Wu, T., Zhao, L., Li, R., Wang, Q., Xie, C., Pang, Q., 2013. Recent ground surface warming and its effects on permafrost on the central Qinghai-Tibet Plateau. Int. J. Climatol. 33 (4), 920–930.

Wu, T., Zhu, X., Wang, P., Adiya, S., Avirmed, D., Dorjgotov, B., Lou, P., 2022b. Climate warming in the Qinghai-Tibet Plateau and Mongolia as indicated by air freezing and thawing indices. Ecol. Indic. 138, 108836.

Yamkhin, J., Yadamsuren, G., Khurelbaatar, T., Gansukh, T.E., Tsogtbaatar, U., Adiya, S., Natsagdorj, S., 2022. Spatial distribution mapping of permafrost in Mongolia using TTOP. Permafr. Periglac. Process. 33 (4), 386–405.

Zhang, T., Frauenfeld, O.W., Serreze, M.C., Etringer, A., Oelke, C., McCreight, J., Chudinova, S., 2005. Spatial and temporal variability in active layer thickness over the Russian Arctic drainage basin. J. Geophys. Res. Atmos. 110 (D16).

Zhang, Y., Cheng, G., Li, X., Han, X., Wang, L., Li, H., Flerchinger, G., 2013. Coupling of a simultaneous heat and water model with a distributed hydrological model and evaluation of the combined model in a cold region watershed. Hydrol. Process. 27 (25), 3762–3776.

Zhang, P., Jeong, J.H., Yoon, J.H., Kim, H., Wang, S.Y.S., Linderholm, H.W., Chen, D., 2020. Abrupt shift to hotter and drier climate over inner East Asia beyond the tipping point. Science 370 (6520), 1095–1099.

Zscheischler, J., Martius, O., Westra, S., Bevacqua, E., Raymond, C., Horton, R.M., Vignotto, E., 2020. A typology of compound weather and climate events. Nat. Rev. Earth Environ. 1 (7), 333–347.